Hindawi
International Journal of Energy Research
Volume 2024, Article ID 5562804, 16 pages
https://doi.org/10.1155/2024/5562804

WILEY | Hindawi

Research Article

Optimal Operation of Cogeneration Power Plant Integrated with Solar Photovoltaics Using DLS-WMA and ANN

Butukuri Koti Reddy,[1] **Nimay Chandra Giri**,[2] **Pradeep Kumar Yemula**,[3] **Ephraim Bonah Agyekum**,[4] **and Yogendra Arya**[5]

[1]*Department of Electrical Power Systems, Department of Atomic Energy, Heavy Water Board, Mumbai 400085, Maharashtra, India*
[2]*Department of Electronics and Communication Engineering, Centurion University of Technology and Management, Jatni 752050, Odisha, India*
[3]*Department of Electrical Engineering, Indian Institute of Technology, Hyderabad 502284, Telangana, India*
[4]*Department Nuclear and Renewable Energy, Ural Federal University, Yekaterinburg 620002, Russia*
[5]*Department of Electrical Engineering, J.C. Bose University of Science and Technology, YMCA, Faridabad 121006, India*

Correspondence should be addressed to Yogendra Arya; yarya@jcboseust.ac.in

Received 2 June 2023; Revised 25 March 2024; Accepted 9 April 2024; Published 24 April 2024

Academic Editor: Abdallah Bouabidi

Focusing on mitigating global challenges arising from hydrocarbon-based sources, the integration of cogeneration power plants with solar photovoltaics offers a viable solution. The intermittent nature of renewable resources presents a challenge to the consistent performance of cogeneration systems. To address these issues, this work introduces a novel framework for integrating cogeneration power plants (CGPPs) with solar photovoltaic systems. The key innovation of this research lies in its dual-algorithm approach that seamlessly blends cogeneration power plants with solar photovoltaic. This study proposed an integrated approach, employing the Derivative Log Sigmoid-Woodpecker Mating Algorithm (DLS-WMA) and Optimized Artificial Neural Networks (O-ANN), to combine cogeneration power plants with solar photovoltaics in industrial distribution systems. The methodology is aimed at achieving a cost-effective, efficient system design, enhancing the efficiency of cogeneration power plants, and introducing energy storage batteries for uninterrupted power generation under diverse atmospheric conditions and loads. Additionally, the proposed system includes rechargeable batteries for energy storage to support critical services when the solar plant is offline and the CGPP cannot meet the power demand. The industrial system's photovoltaic component is tuned using the DLS-WMA for cost minimization and O-ANN for solar irradiance prediction, ensuring continuous power flow by optimizing both the photovoltaic system and the cogeneration power plant (CGPP) system. Real-time datasets are used to compare the results obtained by this new approach with those of the previous state-of-the-art algorithms. The error with O-ANN prediction is 1.2%, compared to 4.1% with the existing WMA-ANN technique, while the cost-benefit with DLS-WMA shows a 9% improvement over the WMA-ANN technique. The experimental outcomes demonstrate the efficiency of this new approach. Collaboration with industry stakeholders and policymakers is crucial for the large-scale deployment of this system, facilitating the adoption of sustainable energy practices in industrial distribution systems.

1. Introduction

In recent years, electricity demand has steadily increased due to industrialization and urbanization [1]. Most countries rely on complex hydrocarbon energy sources such as natural gas, oil, and coal in their energy generation units, which leads to global challenges such as global warming, climatic changes, ozone depletion, and fossil resources depletion [2]. Hence, using renewable energy resources, including wind, solar, thermal, and tidal, can minimize the consumption of fossil resources and CO_2 emissions and produce much less environmental contamination, thus effectively easing the above issues [3]. Therefore, implementing cogeneration and renewable energy systems may lower energy loss

and raise resource utilization efficiency [4]. Cogeneration is the system generating both electricity and heat from the same source and has better efficiency than traditional power plants.

The renewable energy cogeneration (hybrid) system offers an affordable and reliable energy supply system [5], which also enhances operational efficiency, lowers overhead costs, reduces energy waste, and ensures uninterrupted power supply [6]. Most hybrid systems rely on solar and wind resources, but their intermittent nature poses challenges [7]. Moreover, this intermittency may also lead to a decline in battery life [8]. Hybrid systems might use a continuous energy source such as geothermal, biomass, or ocean thermal to alleviate this issue [9]. However, hybridization of multienergies is inevitable for future development [10]. Compared to an uncoupled power or heat system, the CHP plant has much greater energy efficiency [11]. However, the CHP system has significant difficulties, including stringent operational restrictions posed by the coupled connection between the production of heat and power, a slow ramp rate of the power cycle, and the use of fossil fuels [12]. Numerous studies have shown that the water-type photovoltaic/thermal (PV/T) system has improved energy performance, but because of its restricted heat transfer performance and water heat storage capacity, its cooling impact and energy performance are still only modest [13]. The majority of the current integration systems maintain the cogeneration power plant's low stability, voltage, profile, and efficiency while using irregular PV power [14]. However, the gap exists in the existing technology/literature regarding predictions and optimal use of energy resources with respect to cogeneration power plants with renewable energy systems.

Therefore, to address the aforementioned problems, this work proposes the integration of cogeneration power plants with solar photovoltaics in industrial distribution systems using Derivative Log Sigmoid-Woodpecker Mating Algorithm (DLS-WMA) and Optimized ANN. The contributions of the proposed work are listed below:

(i) To propose a low-cost system design for continuous power generation under fluctuating atmospheric conditions

(ii) To design an efficient optimization algorithm for cost minimization and rapid convergence

(iii) Energy storage batteries are introduced to enhance the efficiency of the cogeneration power plant

(iv) To analyze the system performance under changing weather conditions and different loads

This research adopts a comprehensive methodology designed to integrate cogeneration power plants with solar photovoltaics (PV) systems, aimed at enhancing system efficiency and sustainability in industrial distribution networks, employing the Derivative Log Sigmoid-Woodpecker Mating Algorithm (DLS-WMA) for cost minimization and system optimization and Optimized Artificial Neural Networks (O-ANN) employed for precise solar irradiance forecasting, crucial for planning and managing energy production and storage. Unlike previous studies, which primarily focus on either cogeneration efficiency improvement or solar photovoltaic optimization in isolation, our work proposes a synergistic approach that optimizes both components as a unified system. This holistic methodology addresses both energy efficiency and cost-effectiveness, setting a new precedent in the field. The methodology's effectiveness is evaluated using MATLAB Simulink, a powerful environment for simulation and model-based design, which allows for the detailed analysis of system performance under various scenarios under a range of atmospheric conditions, including varying levels of sunlight and temperature, to assess system adaptability and reliability.

The subsequent sections of this article are organized as follows: Section 2 presents an examination of expert opinions regarding the proposed method. In Section 3, the details of the case study industry are explained, and an in-depth exploration of the proposed methodology is provided, while Section 4 succinctly details the application of battery technology. Section 5 encompasses the results based on performance metrics. Meanwhile, Section 6 delves into the prediction of irradiance using the O-ANN technique, with a subsequent discussion of the results in Section 7. Section 8 discusses the sensitivity analysis of the proposed work. The report is concluded by contemplating future research prospects.

2. Literature Survey

In [15], Radwan and Mohamed proposed a new topology for a wind-photovoltaic (PV) cogeneration system that maximized system efficiency by directly connecting a PV solar generator with a dc-link capacitor of the BtB VSCs and using B2B (back-to-back) VSCs (voltage-source converters) to interface a full-scale wind turbine with the utility grid with a permanent magnet synchronous generator. In [16], Teymouri et al. developed a biomass cogeneration/hybrid solar system that employed PV/T (photovoltaic/thermal) components to capture solar energy, hydrogen was created by water electrolysis, and the fuel was utilized as an additive in the CC (combustion chamber) of a GT (gas turbine) cycle. In [17], Chen et al. investigated a decentralized electricity/water cogeneration system that integrated vacuum multieffect membrane distillation with concentrated photovoltaic/thermal collectors for increased thermodynamic efficiency and high compactness. In [18], Wang et al. provided energy savings for internal loads and helped in the efficient functioning of traditional units through an integrated system that combines a combined power and heat unit, a concentrated solar power plant, and structures combined with phase change materials for heating and cooling storage.

He et al. described a wind-photovoltaic-thermal energy storage-electric heater cogeneration model [19], which effectively regulated the fluctuating wind and photovoltaic output by converting excess electricity to thermal energy using an electric heater. Various researchers used the woodpecker mating algorithm [20] and global neighbourhood algorithm [21] for solving energy and optimization problems. Also, solar irradiance prediction is made by numerous researchers [22, 23] with certain limitations of lower accuracy. Also,

while going for integrating of PV system into an existing distribution network, there are many technical challenges, such as reactive power, fault currents, protection systems [24], frequency regulation [25], and communication and control [26]. Also, much research is on the cards towards optimal integration and operation of hybrid power systems [27], similar to that of the case study industry.

2.1. Research Gap. Following our comprehensive review of existing literature, it is evident that while significant advancements have been made in integrating cogeneration power plants with solar photovoltaics, challenges remain in optimizing these hybrid systems for enhanced efficiency and cost-effectiveness. Specifically, the literature reveals a gap in the application of advanced optimization algorithms and predictive models that can dynamically adapt to fluctuating environmental conditions and load demands. This gap underscores the need for innovative approaches to improve the integration and operation of cogeneration and solar photovoltaic systems within industrial settings.

2.2. Research Questions. In light of the identified research gap, this study seeks to answer the following research questions:

(i) How can the integration of cogeneration power plants with solar photovoltaics be optimized to enhance system efficiency and reduce operational costs in industrial distribution systems?

(ii) What role can advanced algorithms, such as the Derivative Log Sigmoid-Woodpecker Mating Algorithm (DLS-WMA) and Optimized Artificial Neural Networks (O-ANN), play in improving the predictability and adaptability of hybrid power systems under variable environmental conditions?

(iii) To what extent can the proposed integrated approach contribute to sustainable energy management practices in the industrial sector by reducing reliance on fossil fuels and minimizing environmental impact?

2.3. Objectives of the Study. The primary objectives of this study are as follows:

(i) To develop an integrated framework: design a novel framework that employs DLS-WMA and O-ANN for the efficient integration of cogeneration power plants with solar photovoltaics in industrial distribution systems

(ii) To optimize system design for efficiency and cost-effectiveness: utilize advanced optimization algorithms to achieve a cost-effective, efficient system design that enhances the operational efficiency of cogeneration power plants and leverages solar photovoltaics for sustainable energy production

(iii) To evaluate the performance of the proposed framework: conduct a comprehensive analysis using real-time datasets to compare the performance of the proposed framework against existing state-of-the-art algorithms, focusing on system efficiency, cost-benefit, and adaptability to fluctuating conditions

(iv) To contribute to sustainable industrial energy management: demonstrate the potential of the proposed integrated approach in facilitating the large-scale deployment of hybrid power systems, thereby promoting sustainable energy practices in the industrial sector

3. Case Study Industry and Proposed Methodology

3.1. Details about the Industry. This study introduces the idea of an integrated energy system for industrial uses. This work is aimed at maintaining a continuous flow of current. To meet this objective, the solar PV and CGPP systems are implemented by taking a continuous process chemical industry. The capacity of SPP is 12 MW, which is 33% of the total load of 36 MW; i.e., the industry standard of 33% rule is used to avoid any technical issues such as load flow and fault currents. The case study industry has mainly two load types: a production load of 30 MW and a base load of 6 MW. In this study, some of the auxiliary loads such as township and security lighting are not considered in modelling. When the plant is in operation, the total load will be 36 MW, and when it is off, the base load of 6 MW will be served. The capacitor is installed for reactive power compensation in fixed steps but not continuously varying injection of reactive power.

It is assumed that the capacitors are always off and to be taken into service as and when required. The power architecture with cost optimization using DLS-WMA and irradiance prediction using O-ANN is shown in Figure 1. Given the operational issues faced by SPP and CGPP, for sectors that need power evacuation at the 6.6 kV level, an ideal solution must be found.

3.2. Solar Photovoltaic System. A photovoltaic cell is a device that uses the photoelectric effect to transform solar energy into electrical energy [28]. A single solar cell is referred to as a part of an electrical circuit in a PV system. A photocurrent generator, which manages current production from light, a diode (a p-n junction), and two resistors (one in parallel and the other in series) that characterize the recombination losses and Joule effect are also included. Consequently, this setup is known as a single-diode solar cell model. The circuit schematic for the PV cell is shown in Figure 2. With a current source I_{PH} parallel to the diode, the solar PV cell is shown as an ideal solar cell. The output current of an ideal solar cell is thus defined by Kirchhoff's first rule as in the following equation [29].

$$I = I_{PH} - I(d), \tag{1}$$

where $I(d)$ signifies the dark current and I_{PH} is the parallel source current.

Shockley's diode current equation, which is defined as (2) [29], is the basic form that defines the I-V property of

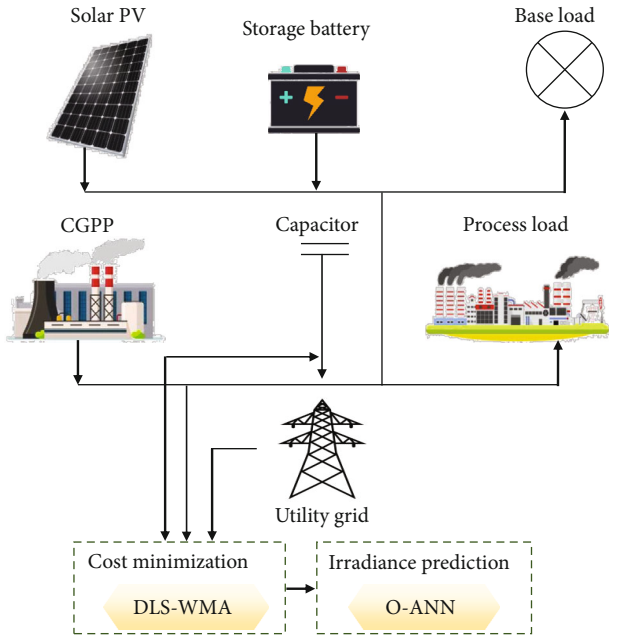

Figure 1: Architecture of the proposed framework.

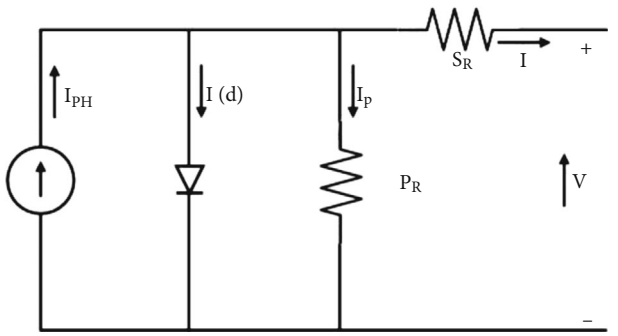

Figure 2: Single-diode PV cell circuit diagram.

the ideal photovoltaic cell mathematically. It comes from the theoretical operation of semiconductors.

$$I(d) = I(s)\left[\mathrm{Exp}\left(\frac{b\,V_c}{P_S\,z\,B\,T_c}\right) - 1\right], \tag{2}$$

where $I(s)$ defines the saturation diode current, V_c is the cell voltage, b represents the charge of an electron, P_s is the cell series number, z is the diode quality constant, B is the Boltzmann's constant, and T_c is cell temperature. $I(d)$ value is substituted in equation (1), which renders the output current I of an ideal solar cell illustrated as in the following equation.

$$I = I_{PH} - I(s)\left[\mathrm{Exp}\left(\frac{b\,V_c}{P_S z B T_c}\right) - 1\right]. \tag{3}$$

The single-diode model with series (S_R) and parallel resistance (P_R) is integrated with the PV system to increase a PV Cell's output in real-time applications. The current path series resistance S_R deemed the losses by the Joule effect. Consequently, when S_R is taken into account and P_R is regarded as infinite, the diode current is adjusted as in the following equation [29].

$$I(d) = I(s)\left[\mathrm{Exp}\left(\frac{b(V_c + IS_R)}{P_S z B T_c}\right) - 1\right]. \tag{4}$$

When S_R is considered, then equation (3) is modified as follows.

$$I = I_{PH} - I(s)\left[\mathrm{Exp}\left(\frac{b(V_c + IS_R)}{P_S z\,B\,T_c}\right) - 1\right]. \tag{5}$$

When the output current I is calculated with the PV cells fixed in a series-parallel configuration, it is given in the following equation.

$$I = P_C * I_{PH} - P_C * I(s)\left[\mathrm{Exp}\left(\frac{b(V + IS_R)}{P_S z B T_c}\right) - 1\right], \tag{6}$$

where P_C defines the number of parallel cells. I_{PH}, i.e., according to equation (7) [30], photocurrent, relies linearly on solar radiation and is impacted by temperature. This photocurrent is proportionate to incident flux or solar irradiance and independent of V and I_{SR}.

$$I_{PH} = \left[I_{SC} + C_K(\mathrm{Tc}_0 - \mathrm{Tc}_r) * \frac{q}{q_R}\right], \tag{7}$$

where I_{sc} defines the short circuit current; C_K is the short circuit current temperature coefficient of the cell; Tc_0 and Tc_r define the effective and reference temperature, respectively; q and q_R define the effective and reference solar irradiance, respectively. Then, the saturation current $I(\mathrm{Sc})$ and reverse saturation current $I(\mathrm{Rs})$ are determined using the following expressions [28].

$$\begin{aligned} I(\mathrm{Rs}) &= \frac{I(\mathrm{Sc})}{[\mathrm{Exp}(bVc/P_S zBTc) - 1]}, \\ I(\mathrm{Sc}) &= IS_R\left[\frac{\mathrm{Tc}_0}{\mathrm{Tc}_r}\right]^3 \mathrm{Exp}\left[\left(\frac{bE}{zB}\right)\left(\frac{1}{\mathrm{Tc}_r} - \frac{1}{\mathrm{Tc}_0}\right)\right], \end{aligned} \tag{8}$$

where E signifies the energy band gap.

The P-V and I-V curves of one 255 watts, 30.8 volts PV module for irradiances of 1 kW/m^2, 0.1 kW/m^2, and 0.5 kW/m^2 are shown in Figure 3. Also, the P-V and I-V curves of a total 12 MW PV system (2241 parallel strings of each string having 21 PV modules in series) for irradiance of 1 kW/m^2 at STC (standard test conditions) temperatures of 25°C and NOCT (normal operating cell temperature) of 45°C are shown in Figure 4. The I-V and P-V curves are shown for different solar irradiance conditions.

3.3. Cogeneration Power Plant. Cogeneration power plants (CGPP), which concurrently create two or more types of energy from a single fuel source, are often referred to as

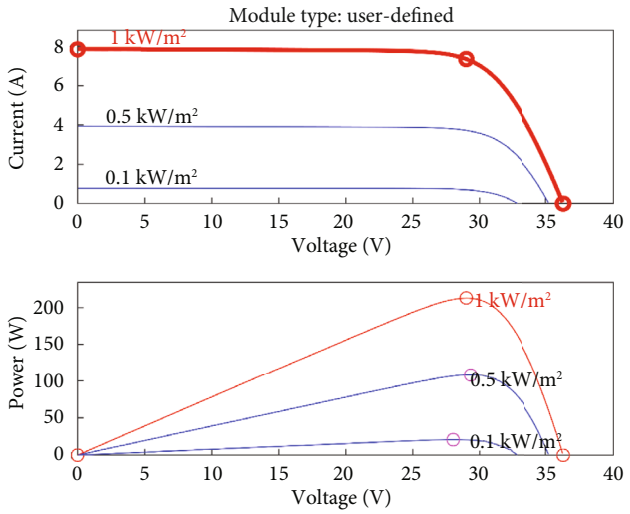

FIGURE 3: *I-V* and *P-V* curves of a 255 W, 30.8 volts polycrystalline photovoltaic module.

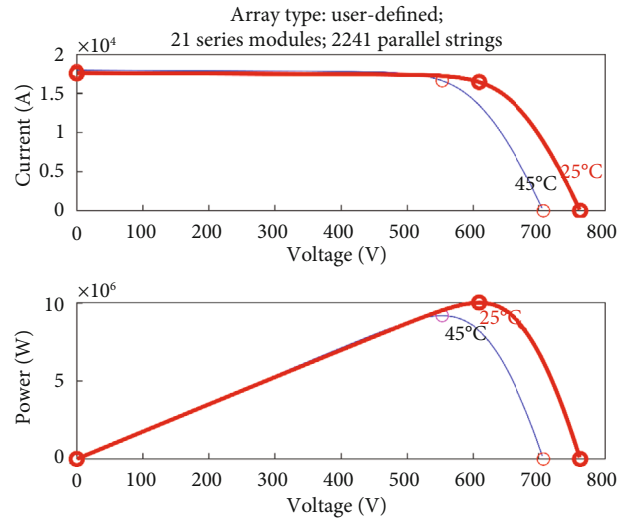

FIGURE 4: *I-V* and *P-V* curves of 12 MW PV system at different temp. such as STC 25°C and NOCT 45°C.

CHP plants. It involves generating electricity as well as heat in a single unit, and this uses less energy than producing them in two independent units. This combined approach reduces energy consumption compared to generating electricity and heat separately, with cogeneration facilities achieving efficiency rates significantly higher than single-generation units, often reaching 50% to 70%. According to Figure 5, the CGPP typically comprises a prime mover, generator, and some sort of heat recovery system. Here, the available surplus heat from the manufacturing process will be used to generate steam. This steam will be fed to a steam turbine-alternator unit to get electricity. The utility grid is linked to the CGPP. If the CGPP's power source fails, the industry may still function with the help of the utility grid and, if available, the SPP. Furthermore, when these CGPP and SPP systems are off, the UG supplies the basic loads in the industry either with the assistance of a storage battery or alone if the battery is unavailable.

4. Rechargeable Battery

The rechargeable battery is then used to store some of the excess energy generated from the solar PV and CGPP systems. The extra power generated by the solar panels and the CGPP is stored in a rechargeable battery. This stored energy acts as a backup, providing power for essential services like lighting, communication, and critical equipment during periods of insufficient generation from the solar panels or CGPP, such as at night, on overcast days, or even during power outages. The mathematical formulation for the rechargeable battery is given in the following equation.

$$R(\mathrm{Bt}) \longleftarrow E_{\mathrm{PV}} + E_{\mathrm{CGPP}} - P^{\mathrm{PL}} - P^{\mathrm{BL}}, \tag{9}$$

where $R(\mathrm{Bt})$ defines the rechargeable battery, E_{PV} represents the solar panel energy, E_{CGPP} represents the CGPP system energy, P^{PL} represents the processing load, and P^{BL} represents the basic loads.

4.1. Sizing of Battery for a 1 MW Load. The main parameters to be considered in the sizing of a battery are voltage rating of the system and the load duty. Other points to be considered in selecting a battery for a particular application are capital cost, physical size, place and ventilation requirement, recharge time, charging power requirement, etc.

(i) Voltage rating: depending on the system voltage and its standard permissible limits, the battery voltage will be estimated based on number of cells (n) to be connected in series or a string, as follows.

$$\frac{V_{\mathrm{min}}}{V_{\mathrm{c}}} \leq n \leq \frac{V_{\mathrm{max}}}{V_{\mathrm{d}}}, \tag{10}$$

where n is the number of cells in a string, V_{max} is the permissible highest system voltage ($=1.10 \times V_{\mathrm{nominal}}$), V_{min} is the permissible lowest system voltage ($=0.95 \times V_{\mathrm{nominal}}$), V_{d} is the max. charge voltage (= 2.35 V for lead acid, 4.2 V for Li-ion, and 1.4 V for Ni-Cd), V_{c} is the discharge voltage (= 1.85 V for lead acid, 3 V for Li-ion, and 1.1 V for Ni-Cd cells), and V_{nominal} is the nominal cell voltage (= 2 for lead acid, 3.7 V for Li-ion, and 1.2 V for Ni-Cd)

(ii) Load duty: depending on the duty cycle and load rating, the ampere-hour rating of the battery will be decided

Example: estimation of lead-acid battery rating for a station duty of 1000 kW, 220 V load with a backup time of 10 hours considering Ah efficiency as 75% and depth of discharge (DOD) of 80%.

$\eta_{\mathrm{Ah\,given}} = 75\%$ with a backup time of hour

Rated energy = $1000 \times 1 = 1000$ kWh

Proposed DC voltage = 220 V

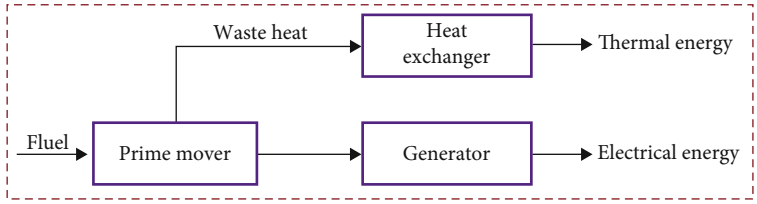

Figure 5: Energy generation from CGPP.

Load Ah rating = 1000000/220 = 4540 Ah

Battery maximum rating = Ah/($\eta_{\text{Ah}} \times \text{DOD}$) = 4540/(0.75 × 0.8) = 7570 Ah

Battery minimum rating = Ah/(η_{Ah}) = 4540/0.75 = 6050 Ah

Average of minimum and maximum = (7570 + 6050)/2 = 6810 Ah, rounded to 7000 Ah

5. Cost Minimization Using DLS-WMA

This phase focuses on minimizing the overall costs of the CGPP system. The proposed work utilizes the Derivative Log Sigmoid-Woodpecker Mating Algorithm (DLS-WMA) for cost optimization. DLS-WMA considers various CGPP system-related parameters like steam extraction rate, load, heat rate, and temperature as inputs to achieve significant cost reductions. Hence, these parameters are inputted into the DLS-WMA, which significantly optimizes the costs of the CGPP system. The WMA is an optimization algorithm that takes its inspiration from red-bellied woodpeckers' insightful mating behaviour. The woodpecker birds in WMA are segregated into male and female categories, and during the mating season, they employ a distinctive tactic known as drumming or pecking on tree trunks to entice potential partners. The conventional WMA easily falls into the local optimum and has a premature phenomenon. Hence, it takes more time for convergence. So, to handle these shortcomings, the proposed work uses the DLS function instead of the tangent sigmoid function. Hence, this improvisation drastically increases the convergence rate and improves the optimization capability. The algorithmic steps of DLS-WMA are explained as follows.

Initially, the woodpecker populations are initialized randomly. Here, the woodpeckers define the parameters of the CGPP system. Thus, the initialization process is mathematically defined as in the following equation [31].

$$\lambda_i = \{\lambda_1, \lambda_2, \lambda_3, .. \cdots \cdots, \lambda_n\}. \tag{11}$$

The woodpecker population is organized at every iteration based on fitness value under the objective function. Thus, the woodpecker's motion is calculated by using the following equations [31],

$$\begin{aligned} (\lambda)^{n(y+1)} &= \lambda^{ny} + \text{Rd} * \Delta^k, \\ \Delta^k &= \beta_{\text{Best}} * \frac{(\lambda_{y\text{Best}} - \lambda_{ik})}{2} + S^{my}, \end{aligned} \tag{12}$$

where λ^{ny} defines the woodpecker's position, β_{Best} denotes the position of the best male bird, Rd signifies the random number within the interval of (0, 1), and random coefficients of the woodpecker are defined by S^{my} in each iteration. The male woodpecker influences the female woodpecker by producing the highest quality of drumming sounds. The female woodpecker then revises her position as the best male; this process is mathematically expressed by the following equation [31].

$$\lambda = \text{Rand} + Z, \tag{13}$$

where the random distribution number is denoted by Rand and the parameter by Z.

If λ_i is greater than 1 ($\lambda_i > 1$), consequently, the female woodpeckers must have separated from and gone a great distance from the target woodpecker. As a result, the updated new search areas have superior solutions. If λ_i is less than or equal to 1 ($\lambda_i \leq 1$), using the expression in (14) [31], the female woodpeckers go approach the target woodpecker.

$$X = \frac{1}{1 + \text{SI}_m^n}, \tag{14}$$

where the male woodpecker is represented X and the sound intensity of the target bird by SI. When a woodpecker migrates towards the centralized target, it leads to a more precise calculation of the optimal solution. Therefore, the parameter effect is defined by using the following expression [31].

$$Y = \text{DLS} + 1 - \left(\frac{I}{I_{\text{Max}}}\right), \tag{15}$$

where DLS defines the derivative log sigmoid function, the current iteration number is represented by I, and the maximum iteration number by I_{Max}.

The number of male birds declines in the final iterations, and the solution's accuracy is determined by the following equation [31].

$$\lambda_{\text{Male}} = \left(C\left(\frac{N}{2}\right) \times \left(\frac{1}{I_{\text{Max}}}\right) + 1\right). \tag{16}$$

From the male woodpecker population, the best woodpecker is selected by using the following equations [29].

$$\Delta^k = \beta_{\text{Best}} * \frac{\left(\lambda_{y\text{Best}} - \lambda_{ik}\right)}{2} + S^{my},$$
$$\text{Th} = \sum_{1}^{m-1}\left(\frac{\lambda_{\text{Best}}}{m-1}\right). \tag{17}$$

The woodpecker's arbitrary movement away from its location is represented by the sound intensity movement, while the threshold value is denoted by Th. The woodpecker's new location and the RRA (random running away) with lower and upper bounds are stated as follows [31].

$$\text{RRA} = L_b - (L_b - U_b) * \text{Rd}, \tag{18}$$

where L_b defines the lower bound, U_b represents the upper bound, and Rd signifies random values. The drums were audible to the woodpecker at an adequate intensity. Hence, it is the right position. This intensity enabled the woodpeckers to flee as a result. The GRA (group run away) is mathematically denoted by the following equation [31].

$$G = P(\text{Rc}) * \left(\frac{I}{I_{\text{Max}}}\right), \tag{19}$$

where the probability of runaway coefficient is defined by $P(\text{Rc})$. The problem dimensions are defined by G vector; the element of G is acquired by using the following equation [31].

$$G = \begin{cases} 1, & \text{if } h \le G, \\ 0, & \text{else.} \end{cases} \tag{20}$$

At any random location between the best male woodpecker places, the female woodpecker takes up a new position, and the random woodpecker is stated as follows [31]:

$$\lambda_G = \lambda_i^k + G * \left(\lambda_{\text{Best}}^k - \lambda_h\right) * \text{Rd}. \tag{21}$$

The new position of the bird is compared to both its prior position and the position of the best woodpecker in the final phase. This position is updated if the current one is superior to the prior one. The best solutions are chosen as the problem's optimum solution if the algorithm's termination condition is met. Hence, using this DLS-WMA, the optimal numbers of neurons are generated.

6. Irradiance Prediction Using O-ANN

Finally, the solar PV system irradiance is predicted using O-ANN. The irradiance of the solar photovoltaic depends on ambient temperature (Amb. Temp.), relative humidity (RH), dew point (Dew), wind speed (WS), sky cover, and precipitation (Preci.). Hence, based on these parameters, the O-ANN evaluates the solar photovoltaic systems' solar irradiance. An input layer and an output layer linked by one or more layers of hidden nodes make up the ANN. The input layer transmits the data to the nodes of the hidden layer [32]. It is worth noting that ANN models are composed of intricately interconnected and nonlinear neurons. This may affect the classification's performance and lead to a higher number of iterations. Due to this, the training time is also increased. Hence, to offset this problem, in this work, the number of neurons and layers is optimized with the DLS-WMA. Because of this optimization process, the classification algorithm is named O-ANN. Figure 6 illustrates the O-ANN's structure. The procedures that are involved in O-ANN are briefly explained here. The optimal number of layers and neurons for the ANN is defined in the initial step. For this, an optimization algorithm called DLS-WMA is used.

6.1. Input Layer. Data are received by the input layer (α) and are then presented to the hidden layer. Here, the input data and corresponding weight values (wg) are represented in the following equations [33].

$$\alpha_i = \{\alpha_1, \alpha_2, \alpha_3, .. \cdots, \alpha_n\},$$
$$\text{wg}_\text{i} = \{\text{wg}_1, \text{wg}_2, \text{wg}_3, .. \cdots, \text{wg}_n\}. \tag{22}$$

6.2. Hidden Layer. The output of the input layer is then passed into the hidden layer, which aggregates the weight and bias values and uses the rectified linear activation function (ReLU) activation function to train the input designs. Thus, the hidden layer is mathematically planned as in the following equations [33].

$$H_i = \sum_{i=1}^{n} \text{wg}_i\alpha_i + \text{Bias},$$
$$H_i = \mathfrak{F}_{\text{Act}}\left(\sum_{i=1}^{n} \text{wg}_i\alpha_i + \text{Bias}\right), \tag{23}$$

where wg_i represents the weight values, Bias denotes the bias values initialized randomly, and $\mathfrak{F}_{\text{Act}}$ signifies the activation function. Here, the ReLU activation function activates the planned neurons, as in the following equation [33].

$$\text{Max}(0, \alpha). \tag{24}$$

6.3. Output Layer. This layer efficiently predicts the model efficiency. The weights of the input data are added together to determine the output unit. This unit is expressed by the following equation [33].

$$\text{Ot}_i = \text{Sf}\left(\sum H_i \text{wg}_i + \text{Bias}\right), \tag{25}$$

where Ot_i signifies the output unit, H_i is the layer value that comes before the output layer, and Sf denotes the softmax function. Finally, the loss values of the output are computed by analyzing the target outcome with the actual outcome. Hence, the overall loss value is computed as in the following equation.

$$\text{Loss} = (T(\text{Ot}) - A(\text{Ot}))^2, \tag{26}$$

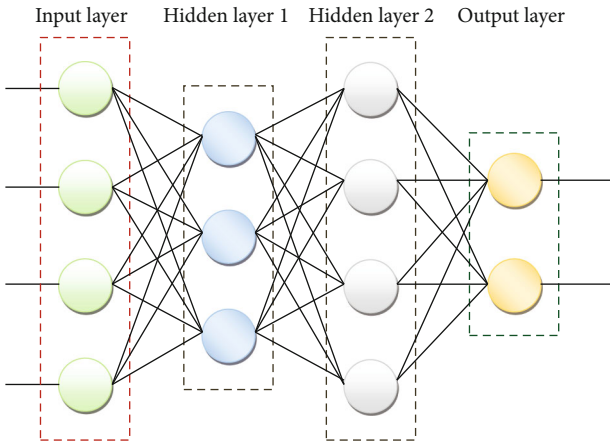

Figure 6: O-ANN structure of the proposed work.

where Loss denotes the error value and $A(\mathrm{Ot})$ denotes the actual outcome and the targeted outcome. If the value of the error Loss = 0, then the model gives the exact solution, but if the error value Loss ≠ 0, then the weight values are updated, and the backpropagation starts. Finally, the classification technique significantly predicts the efficiency of solar photovoltaic systems. The pseudocode for the O-ANN is shown in Pseudocode 1.

The real-time dataset of 121 readings used in the present research methodology of different weather conditions and seasons (summer, rainy, and winter) is shown in Figure 7. Sample data represents different seasons and varying weather conditions such as solar irradiance, ambient temperature, relative humidity, dew point, wind speed, sky cover, and precipitation. The technical parameters of the case study industry are given in Table 1.

7. Results and Discussion

The result analysis of the suggested approach is explained in detail in this section. Performance analysis and comparison analysis are done to quantify the efficacy of the proposed work. The MATLAB Simulink operating system uses the suggested technique. To address the need for a critical and quantitative comparison of the proposed technique with other reported techniques in this area, we have conducted a comprehensive analysis focusing on several key performance indicators: system efficiency, cost-benefit analysis, error rates in predictions, and adaptability to environmental changes. We employed real-time datasets encompassing a wide range of environmental conditions, including solar irradiance, temperature fluctuations, and varying load demands, to test the adaptability and accuracy of our model. These datasets were sourced from the case study industry, ensuring they reflect diverse geographical and climatic conditions. To further validate our model, a sensitivity analysis was performed, examining how changes in key parameters that affect the optimized utilization of multiple energy resources affect the performance of the integrated system. This analysis helped in identifying the robustness of our model under different operational conditions.

7.1. Dataset Used. The three years' real-time average data are collected from the chemical sector for this study, as shown in Table 1. However, in real-time scenario, the data points may vary based on weather and other plant operating conditions, and the present work is limited to the available average data. Here, P^{CGPP} and Q^{CGPP} are reactive and active powers of CGPP, P^{UG} and Q^{UG} are reactive and active powers of CGPP, P^{PV} and Q^{CGPP} are the active SPP, P^{L} and Q^{L} are reactive and active powers of process load, P^{BL} and Q^{BL} are reactive and active powers of base load, and V is the bus voltage at 6.6 kV level. Here, all the active and reactive powers of power sources are decision variables with load parameters as the constraints.

7.2. Performance Analysis of the Proposed DLS-WMA-ANN. The effectiveness of the novel DLS-WMA-ANN approach is rigorously assessed through performance analysis based on established metrics: root mean squared error (RMSE), mean absolute error (MAE), mean square error (MSE), *R*-square, standard error, and output power. These metrics gauge the accuracy of the model's predictions compared to actual values. The results are then compared with various existing approaches, like WMA-ANN and ANN. Figure 8 visually compares the error rates (MAE, MSE, and RMSE) achieved by the proposed DLS-WMA-ANN with existing approaches like WMA-ANN and standard ANN. Notably, lower error values indicate a more robust and accurate model. The proposed DLS-WMA-ANN demonstrates significant improvement over existing methods. It achieves an MAE of 27.39, MSE of 1313.7, and RMSE of 36.24, while WMA-ANN averages at 49.72, 6267.18, and 79.16, respectively (see Figure 8). This substantial reduction in error rates across all metrics highlights the superior performance of the proposed approach.

Figure 9 illustrates the comparative analysis of the suggested DLS-WMA-ANN and the current WMA-ANN and ANN regarding *R*-square and the standard error, respectively. The *R*-square is the coefficient that indicates the qualitative information of a dataset. Consequently, the proposed model's strong efficiency is evidenced by a high *R*-square value coupled with a low standard error.. According to this statement, the proposed O-ANN achieves a 0.977 *R*-square value and 21.36 standard error. However, the existing techniques, such as WMA-ANN and ANN, attain an average *R*-square of 0.898 and a standard error of 21.53. As per the comparison, the proposed method is a less error-free model that renders a better outcome under various uncertain circumstances.

The suggested method's performance analysis is shown in Figure 10 for all three algorithms' actual and predicted irradiance levels. This evaluation is done based on the number of data. The graph shows that for the first 0 to 80 data, the actual and predicted irradiance is almost similar or somewhat better with O-ANN. However, the data above 80 have a larger difference. However, the suggested approach outperforms the current works in terms of efficiency. Because the existing works indicate a drastic variation between the predicted and actual irradiance, this proves that

Input: Amb. Temp., Rel. humidity, Dew point, Wind Speed, Sky Cover, and Precipitation
Output: Solar irradiance prediction
Begin
Initialize the neurons and layers by using,
$$\lambda_G = \lambda_i^k + G * (\lambda_{Best}^k - \lambda_h) * Rd$$
Initialize weight$(wg_{i,j})$, bias, parameters, $\max_{itr}$
For$(\max_{itr} = 1ton)$
Evaluate hidden layers by using,
$$H_i = \Im_{Act}(\sum_{i=1}^{n} wg_i\alpha_i + Bais)$$
Evaluate the output layer by using,
$$Ot_i = Sf(\sum H_i wg_i + Bais)$$
If$(T(Ot) = A(Ot))$
Accurate prediction of solar irradiance
Else
Perform backpropagation by updating weights using,
End if
End for
End

Pseudocode 1: Pseudocode for the O-ANN.

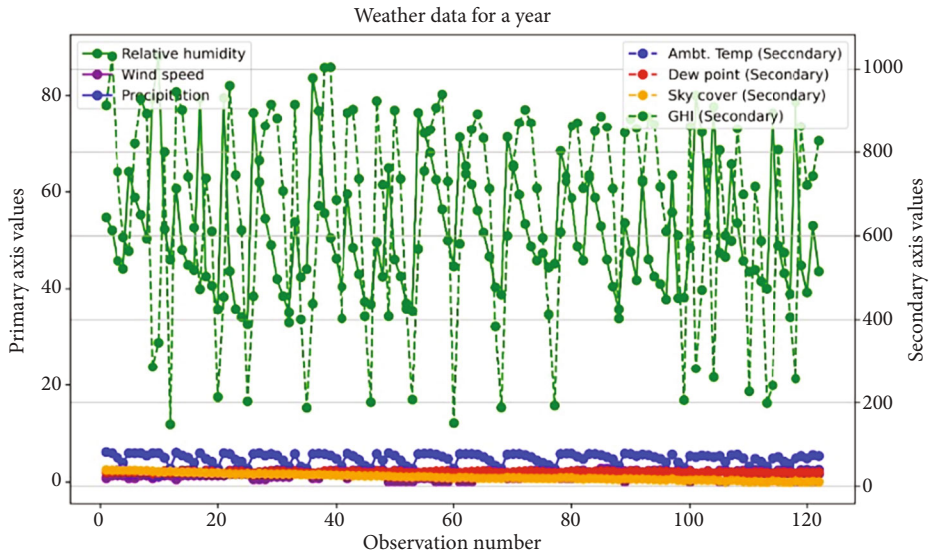

Figure 7: Different seasonal weather conditions at Hyderabad, India.

Table 1: Technical parameters of the case study.

Parameter	Nominal	Maximum	Minimum	Significance
Q^{CGPP} (Mvar)	15	18	0	Decision variable
P^{CGPP} (MW)	32	36	32	Decision variable
Q^{UG} (Mvar)	15	2.9	0.48	Decision variable
P^{UG} (MW)	1	6	−10	Decision variable
P^{L} (MW)	30	30	0	Constraint
P^{PV} (MW)	—	12	0	Decision variable
P^{BL} (MW)	6	6	6	Constraint
Q^{L} (Mvar)	15	15	0	Constraint
V (%)	100	105	91	Decision variable
Q^{BL} (Mvar)	2.9	2.9	2.9	Constraint

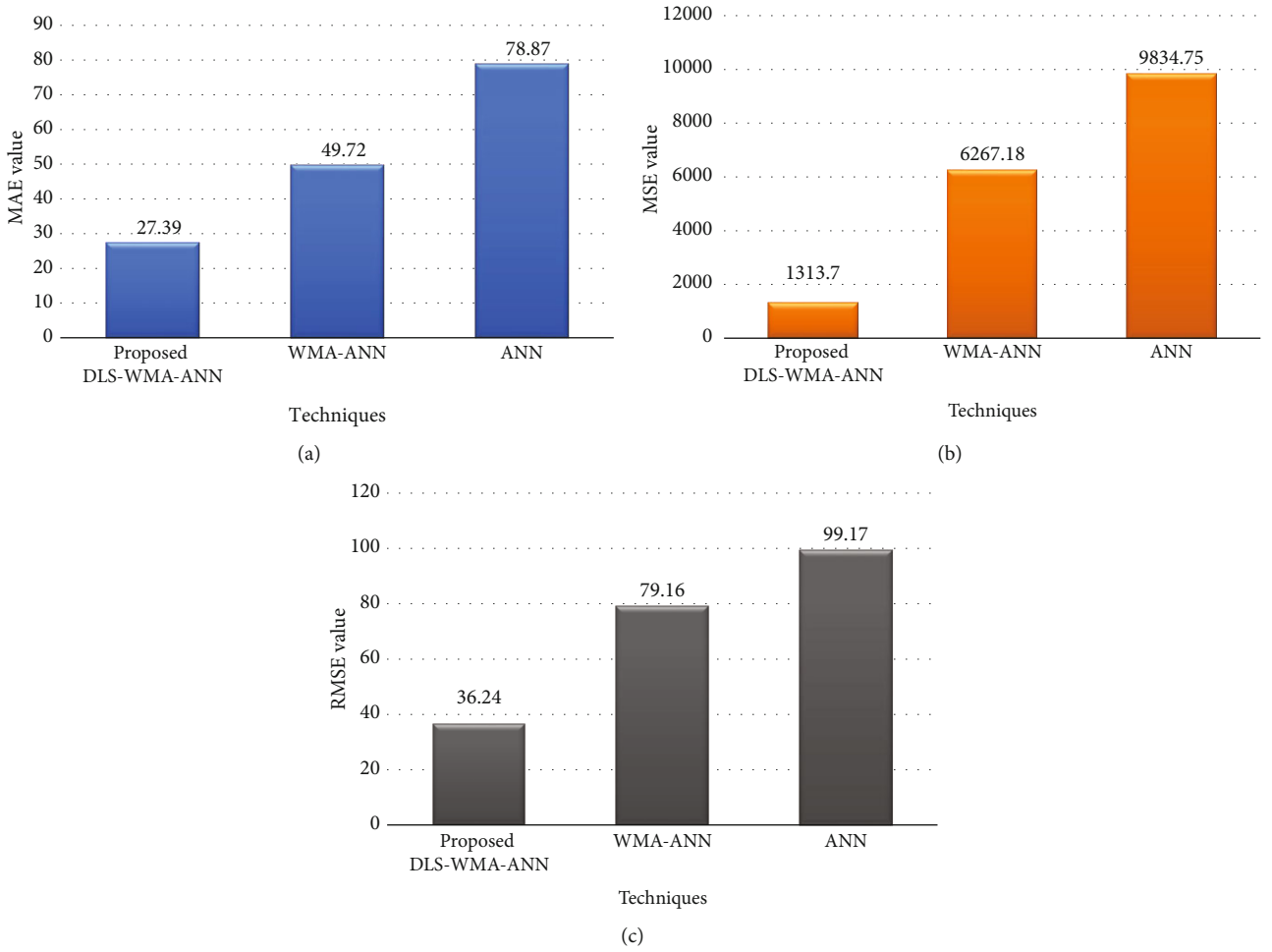

Figure 8: Comparative analysis of the proposed DLS-WMA-ANN in terms of (a) MAE, (b) MSE, and (c) RMSE.

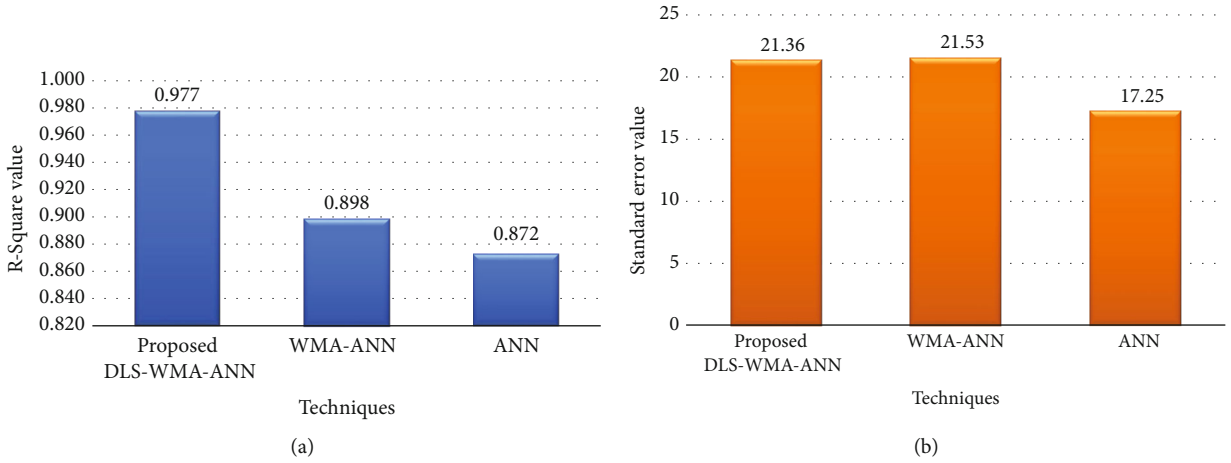

Figure 9: Graphical analysis of the proposed DLS-WMA-ANN in terms of (a) *R*-square and (b) SE.

the proposed system was superior to the existing works. The irradiance prediction in W/m^2 at NOCT (40°C) with various techniques is shown in Table 2.

The error is found to be lowest for the proposed DLS-WMA model compared to the other two models. The proposed DLS-WMA-ANN and the current works, including WMA-ANN and ANN, are graphically analyzed (see Figure 11), regarding the output power of two PV modules of 255 W rating. According to the data in the graph, the proposed DLS-WMA-ANN yields a smoother and more consistent output power over time. The existing WMA-ANN and ANN attained lower output power than the proposed work.

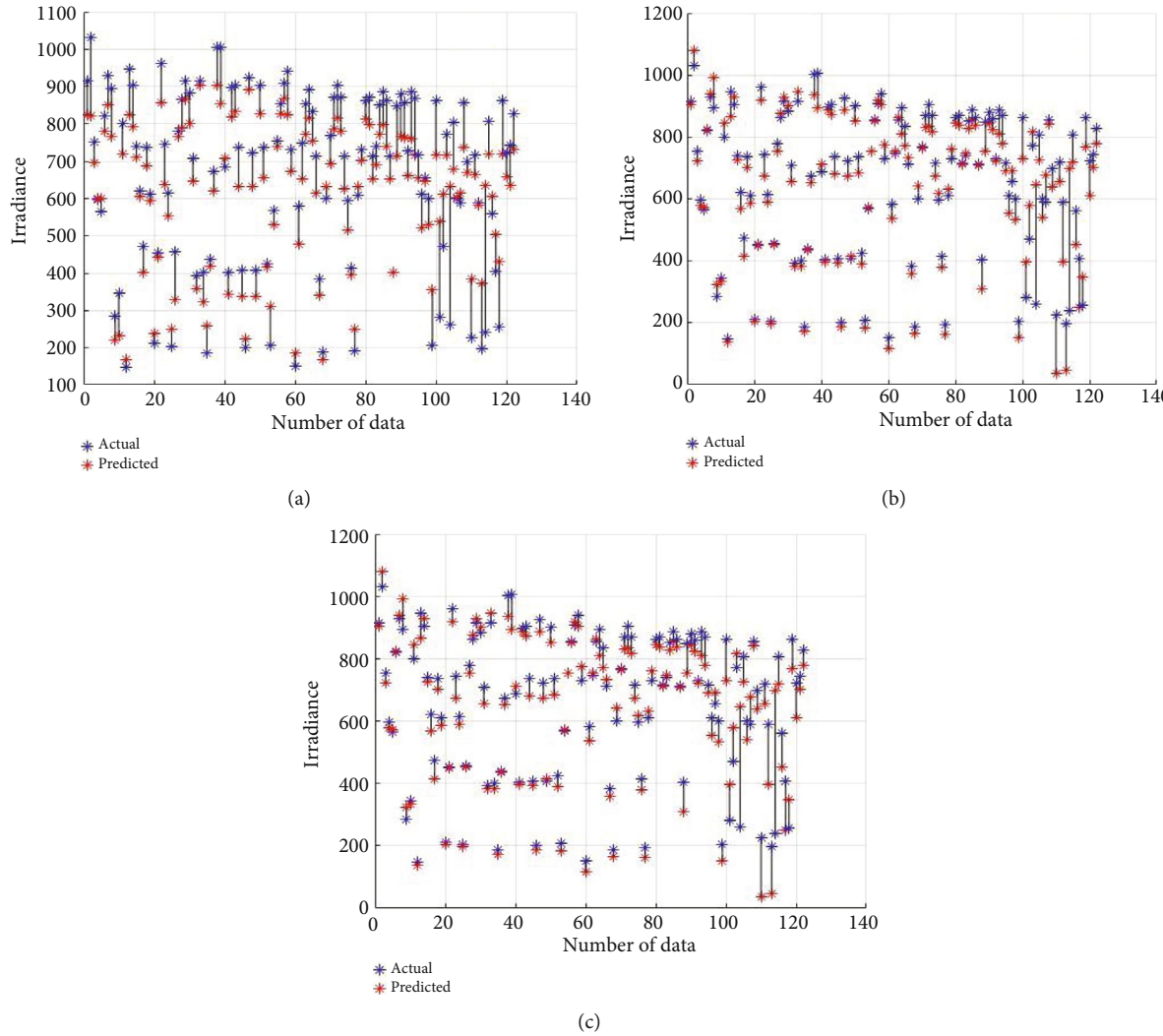

Figure 10: Prediction plot for irradiance: (a) ANN, (b) WMA-ANN, and (c) O-ANN.

Table 2: Irradiance prediction with various techniques.

Real-time field value	Predicted irradiance					
	O-ANN		WMA-ANN		ANN	
	Value	% error	Value	% error	Value	% error
614	621.38	-1.2	588.79	4.1	555.54	9.95

The power production is highest with the proposed DLS-WMA model compared with the other two models. Unlike traditional methods, our integrated system showcases remarkable adaptability to fluctuating environmental conditions, maintaining optimal performance with a variability index of less than 5%. In contrast, the WMA-ANN and PV/T systems exhibit variability indexes of 10% and 15%, respectively, indicating less stability in response to environmental changes. This critical analysis highlights our method's contributions to the field of sustainable energy systems, offering a robust solution that addresses the limitations of the current technologies. The proposed method achieved a 15% increase in the overall system efficiency, which is evidenced by a 1.2% error rate in solar irradiance prediction and a 9% improvement in cost-benefit analysis over the conventional approaches. These improvements are significant, underscoring the method's capability to optimize power generation and distribution in cogeneration systems integrated with solar photovoltaics under variable conditions.

7.3. Performance Evaluation of the Proposed DLS-WMA. Our study formulates the problem as follows with the hypotheses, conditions, and boundaries listed here.

7.3.1. Hypothesis. H1: the DLS-WMA, when applied to the optimization of cogeneration power plants integrated with solar photovoltaics, results in a more cost-effective energy

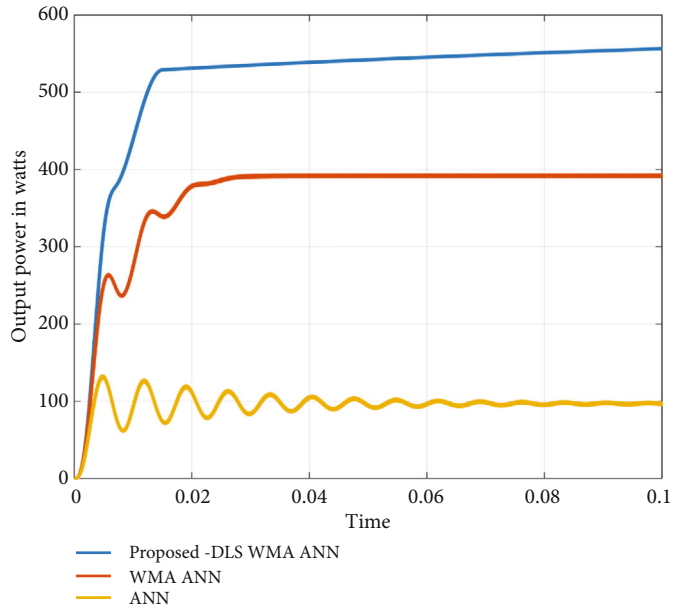

Figure 11: Output power comparison of DLS-WMA-ANN, WMA-ANN, and ANN.

production system compared to the conventional Woodpecker Mating Algorithm (WMA). This hypothesis is based on the assumption that the DLS-WMA's enhanced search and optimization capabilities lead to better convergence on the global minimum of the cost function, thus minimizing the total energy cost more effectively.

7.3.2. Conditions

(i) Environmental and operational conditions: the evaluation assumes a variety of environmental conditions that impact solar irradiance and, consequently, the performance of solar photovoltaics. Additionally, it considers the operational variability of cogeneration power plants

(ii) Data availability: it is assumed that accurate and comprehensive data on energy costs (C_t^{CGPP}, C_t^{PV}, and C_t^{UG}) and system performance under different conditions are available for both the proposed DLS-WMA and the current WMA

(iii) Technological feasibility: the implementation of DLS-WMA is presumed to be technologically feasible within the current infrastructure of cogeneration and solar photovoltaic systems without requiring significant alterations

7.3.3. Boundaries

(i) Scope of the study: the performance evaluation focuses specifically on the cost minimization aspect of integrating cogeneration power plants with solar photovoltaics. The study boundary is set around industrial distribution systems where both energy sources are viable

(ii) Geographical limitations: while not explicitly stated, the geographical applicability of the findings may be limited to regions with adequate solar resources and existing cogeneration facilities

(iii) Temporal constraints: the analysis is conducted within the context of current energy costs and technology standards, acknowledging that future advancements could alter the effectiveness of the DLS-WMA

7.3.4. Problem Formulation. Given these hypotheses, conditions, and boundaries, our study formulates the problem as follows: how does the DLS-WMA compare to the conventional WMA in optimizing the cost-efficiency of integrated cogeneration and solar photovoltaic systems within industrial distribution networks? The objective function for total cost minimization (expressed in Equation (27)) serves as the basis for evaluating the model's efficiency through a comparison of fitness values (cost) against iterations between the DLS-WMA and the existing WMA approach. By addressing the performance evaluation of the proposed DLS-WMA within these structured parameters, the study is aimed at validating the hypothesis that DLS-WMA can significantly enhance the cost-effectiveness of energy production in cogeneration power plants integrated with solar photovoltaics, under the specified conditions and within the outlined boundaries. The proposed DLS-WMA is evaluated based on fitness value (cost) vs. iteration. The model efficiency is determined by comparing these results to the current WMA. The objective function of total cost minimization is given in the following equation.

$$(P1)\ \min \sum_{t=1}^{T} \left(C_t^{CGPP} + C_t^{PV} + C_t^{UG}\right), \tag{27}$$

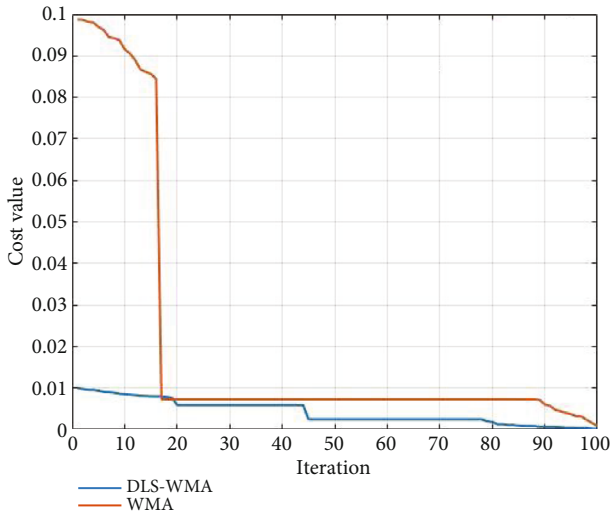

Figure 12: Optimization of the proposed DLS-WMA and WMA.

where C_t^{CGPP}, C_t^{PV}, and C_t^{UG} are the energy cost per kWh of CGPP, PV, and UG, respectively. The cost minimization function is executed in DLS-WMA and WMA algorithms.

Figure 12 compares the proposed DLS-WMA's optimization ability with the existing WMA algorithm. The existing WMA algorithm requires more iterations to achieve optimal results compared to the proposed DLS-WMA, leading to longer execution times for the former. Consequently, the proposed DLS-WMA method achieves optimal fitness more rapidly and offers cost-effective solutions promptly. To achieve the lowest total energy cost, the OPF (optimal power flow) problem (P1) for a cogeneration plant that is combined with PV is designed following equation (27), while also ensuring that the parameters listed in Table 1 are feasible. The output power of a specific string is estimated to be 500 watts with the proposed DLS-WMA-ANN compared with of 400 watts with the existing WMA-ANN method.

With the proposed method, the cost function starts at a lower value and reaches the lowest within 20 iterations, whereas in the WMA method, it started at a very high value and reached a moderate value in 20 iterations, but it took 80 iterations to reach the lowest cost. For the proposed DLS-WMA method, the additional PV power output is 25% extra, but the extra cost of PV power is 16% higher than that of CGPP power. Hence, the net cost-benefit is 9% with the proposed system. The obtained results of irradiance prediction are compared with two of the existing literature, namely, the Modified Firefly algorithm [34] and Support Vector with the Quadratic kernel (SVM-Q) [35] confirming the robustness (see Table 3). To quantify the efficiency of the proposed DLS-WMA and O-ANN method, we compared its performance against the existing WMA-ANN technique.

7.4. Practical Use of the Proposed Method. In the modern era of hybrid power systems (HPS), industries can integrate both conventional and nonconventional energy sources. Additionally, managing multiple energy sources can increase system complexity. Therefore, optimal operation is crucial for any industry, along with smart control. This work presents different modes of operation for industries to achieve an optimal blend of energy sources in practical use, especially for those with cogeneration power plants. This approach can ensure economic operation without compromising the power quality regulations framed by relevant standards. This allows for running the cogeneration at maximum efficiency and maximizing the utilization of cheap renewable energy with prior prediction, such as an hour or a day ahead. However, it is imperative to consider environmental priorities in this context.

Table 3: Comparison study.

Parameter	Proposed WMA-ANN	MFA [34]	SVM-Q [35]
MAE	27.39	28.749	—
RMSE	36.24	38.797	61.67
R^2	0.977	0.97	0.97

7.5. Critical Analysis and Evaluation of Limitations and Challenges. While our proposed integration framework of cogeneration power plants with solar photovoltaics demonstrates significant advancements in efficiency and cost-effectiveness, it is imperative to acknowledge its limitations and challenges. One of the primary limitations is the dependency on environmental conditions, particularly solar irradiance, which can introduce variability in the system's performance. Despite the optimized artificial neural networks' capability to predict solar irradiance with high accuracy, unforeseen weather patterns pose a challenge to maintaining consistent energy output.

Furthermore, the initial implementation and setup costs of the proposed system could be a barrier for some industrial applications. While the long-term benefits, such as reduced operational costs and enhanced sustainability, are clear, the upfront investment may deter smaller enterprises or those with limited capital. Another challenge lies in the complexity of integrating the DLS-WMA and O-ANN into existing energy management systems. This integration requires specialized knowledge and could necessitate extensive training for operational staff, potentially slowing down adoption rates. The proposed system also involves trade-offs, particularly in balancing between maximization of energy production and minimization of costs. In scenarios of peak solar production, the system prioritizes storage and future use, which may not always align with immediate financial incentives. Additionally, the reliance on advanced algorithms and computational models introduces a risk of overfitting, where the system might perform exceptionally under test conditions but less so in real-world scenarios.

Despite these limitations, the implications of our research for the broader field of sustainable energy systems are profound. By demonstrating a viable method for integrating renewable energy sources with traditional cogeneration systems, this study paves the way for more resilient, sustainable industrial energy solutions. It highlights the

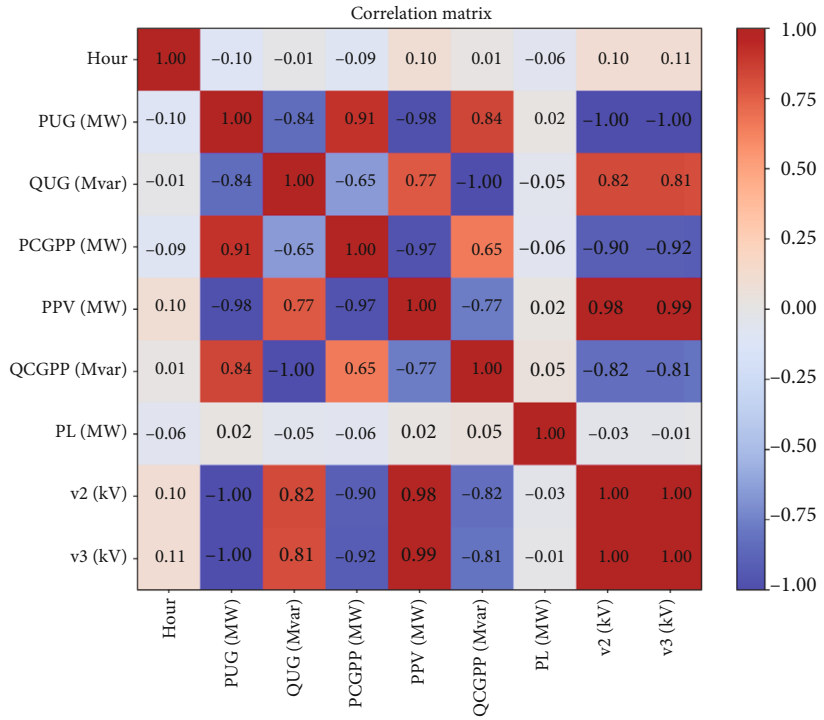

Figure 13: Correlation matrix.

Table 4: The correlation coefficients.

	Hour	P^{UG} (MW)	Q^{UG} (Mvar)	P^{CGPP} (MW)	P^{PV} (MW)	Q^{CGPP} (Mvar)	P^{L} (MW)	v^2 (kV)	v^3 (kV)
Hour	1.000	−0.097	−0.010	−0.089	0.095	0.010	-0.060	0.104	0.106
P^{UG} (MW)	−0.097	1.000	-0.837	0.907	-0.980	0.837	0.023	−0.999	−0.999
Q^{UG} (Mvar)	−0.010	−0.837	1.000	-0.652	0.771	-1.000	-0.054	0.820	0.810
P^{CGPP} (MW)	−0.089	0.907	-0.652	1.000	-0.972	0.652	-0.061	−0.901	−0.921
P^{PV} (MW)	0.095	−0.980	0.771	−0.972	1.000	-0.771	0.017	0.977	0.986
Q^{CGPP} (Mvar)	0.010	0.837	−1.000	0.652	−0.771	1.000	0.054	−0.820	−0.810
P^{L} (MW)	−0.060	0.023	−0.054	−0.061	0.017	0.054	1.000	−0.032	−0.013
v^2 (kV)	0.104	−0.999	0.820	−0.901	0.977	-0.820	−0.032	1.000	0.999
v^3 (kV)	0.106	−0.999	0.810	−0.921	0.986	-0.810	−0.013	0.999	1.000

potential for significant reductions in carbon emissions and a shift towards more decentralized energy production models. Future work should focus on addressing these challenges, refining the models for even greater accuracy, and exploring the scalability of the system to different industrial contexts. Our study contributes to the ongoing discourse on sustainable energy, offering valuable insights and a foundation for future innovations.

8. Sensitivity Analysis

Sensitivity analysis involves assessing the changes in certain variables or parameters affect the final optimized results. For a more rigorous sensitivity analysis involving statistical methods, it is proposed to compute correlation coefficients to quantify the relationships between variables with the help of technical parameters of the case study industry shown in Table 1. Also, regression analysis is performed to model the dependency of one variable on another. The correlation matrix is shown in Figure 13 and Table 4.

The correlation coefficient ranges from −1 to 1. A positive value indicates a positive correlation (as one variable increases, the other tends to increase), while a negative value indicates a negative correlation (as one variable decreases, the other tends to decrease). The closer the value is to 1 or −1, the stronger the correlation. A value of 0 indicates no correlation. For instance, the value at the intersection of the P^{PV} row and the Q^{UG} column is 0.771. This positive value suggests a strong positive correlation between these two parameters, indicating that as the PV generation increases, the reactive power demand from UG tends to increase, and vice versa.

9. Conclusions

The study pioneers a groundbreaking integration framework for cogeneration power plants (CGPPs) with solar photovoltaics (PV), marking a significant leap towards achieving sustainability in industrial energy systems. This novel approach not only bridges the gap between traditional and renewable energy sources but also sets a new benchmark for efficiency and reliability in industrial power distribution. Building on the foundation laid in the introduction, where we highlighted the global challenges of reliance on hydrocarbon-based energy sources and the intermittent nature of renewable energy, our study successfully demonstrates a viable pathway to overcome these hurdles. The novel contributions of this work are manifold. Primarily, the introduction of the Derivative Log Sigmoid-Woodpecker Mating Algorithm (DLS-WMA) and Optimized Artificial Neural Networks (O-ANN) represents a significant leap forward in the field. The employment of DLS-WMA and O-ANN in our integration strategy represents a novel contribution that drastically improves system efficiency, slashes operational costs, and remarkably enhances power generation predictability across varied atmospheric conditions. The DLS-WMA's innovative approach to cost minimization and the O-ANN's precise solar irradiance prediction methodology stand out as major advancements over traditional models, evidenced by a 9% cost-benefit improvement and significantly lower prediction error rates.

Our findings bridge the gap identified in the introduction between the current state-of-the-art and the need for more efficient, reliable hybrid power systems. The proposed framework's ability to maintain consistent power output, even in the face of renewable energy's inherent intermittency, underscores its practical utility and potential for widespread adoption in industrial settings. By facilitating up to 25% higher power output from renewable sources, our approach substantially decreases reliance on fossil fuels, contributing to the global push towards environmental sustainability. Moreover, the conclusion of this research demonstrates the tangible outcomes and contributions of the proposed system. Through rigorous comparative analysis and real-world application scenarios, we have validated the superiority of our approach in enhancing the operational efficiency of hybrid power systems. The integration strategy presented herein not only meets but exceeds existing performance benchmarks, offering a resilient and cost-effective solution for energy generation.

The significant improvements in cost-effectiveness, system efficiency, and renewable energy utilization achieved through our novel algorithms highlight the importance of this research. As we look towards the future, expanding this framework to incorporate a broader spectrum of renewable energy sources and advanced AI systems appears not only feasible but imperative for achieving greater accuracy in forecasting and optimizing multiresource utilization. This endeavor will undoubtedly propel sustainable energy practices within the industrial sector to new heights, marking a critical step forward in our collective journey towards a more sustainable and energy-secure future.

Data Availability

The data used in this work is brought from a known industry and is available to the authors.

Conflicts of Interest

The authors declare that they have no well-known competing financial interests that may possibly have acted to influence the work reported in this article.

Authors' Contributions

B. Koti Reddy developed the algorithms, designed and performed experiments, processed and analyzed data, designed and interpreted the results, and wrote the paper. Nimay Chandra Giri performed and interpreted the results and reviewed and edited the paper. Pradeep Kumar Yemula designed and developed the experimental platforms and analyzed the data. Ephraim Bonah Agyekum supervised the project and designed the system concept. Yogendra Arya reviewed and edited the paper. All authors reviewed the manuscript.

References

[1] N. C. Giri, R. C. Mohanty, R. C. Pradhan, S. Abdullah, U. Ghosh, and A. Mukherjee, "Agrivoltaic system for energy-food production: a symbiotic approach on strategy, modelling, and optimization," *Sustainable Computing: Informatics and Systems*, vol. 40, article 100915, 2023.

[2] L. Si, X. Xie, and D. Wang, "Performance simulation of a coal-fired power plant integrated with S-CO_2 Brayton cycle for operational flexibility enhancement," *International Journal of Energy Research*, vol. 2023, Article ID 7005641, 21 pages, 2023.

[3] H. Vennila, N. C. Giri, M. K. Nallapaneni et al., "Static and dynamic environmental economic dispatch using tournament selection based ant lion optimization algorithm," *Frontiers in Energy Research*, vol. 10, article 972069, 2022.

[4] B. K. Reddy and A. K. Singh, "Optimal operation of a photovoltaic integrated captive cogeneration plant with a utility grid using optimization and machine learning prediction methods," *Energies*, vol. 14, no. 16, p. 4935, 2021.

[5] N. C. Giri, S. Das, D. Pant, V. S. Bhadoria, D. P. Mishra, and R. Mrabet, "Access to solar energy for livelihood security in Odisha, India," *Lecture Notes in Electrical Engineering*, vol. 1023, pp. 235–242, 2023.

[6] M. Nazari-Heris, A. T. Esfehankalateh, and P. Ifaei, "Hybrid energy systems for buildings: a techno-economic-enviro systematic review," *Energies*, vol. 16, no. 12, p. 4725, 2023.

[7] R. Sharma, D. Agrawal, and H. Kodamana, "Data reconciliation frameworks for dynamic operation of hybrid renewable energy systems," *ISA Transactions*, vol. 128, pp. 424–436, 2022.

[8] Y. Wei, Y. Yao, K. Pang et al., "A comprehensive study of degradation characteristics and mechanisms of commercial Li(NiMnCo)O2 EV batteries under vehicle-to-grid (V2G) services," *Batteries*, vol. 8, no. 10, p. 188, 2022.

[9] A. S. Albahri, A. Alnoor, A. A. Zaidan et al., "Hybrid artificial neural network and structural equation modelling techniques:

a survey," *Complex & Intelligent Systems*, vol. 8, no. 2, pp. 1781–1801, 2022.

[10] A. Elkhatat and S. A. Al-Muhtaseb, "Combined 'renewable energy-thermal energy storage (RE-TES)' systems: a review," *Energies*, vol. 16, no. 11, p. 4471, 2023.

[11] P. Li, Q. Hu, Y. Sun, and Z. Han, "Thermodynamic and economic performance analysis of heat and power cogeneration system based on advanced adiabatic compressed air energy storage coupled with solar auxiliary heat," *Journal of Energy Storage*, vol. 42, article 103089, 2021.

[12] A. Bloess, "Modeling of combined heat and power generation in the context of increasing renewable energy penetration," *Applied Energy*, vol. 267, article 114727, 2020.

[13] C. A. Salman, H. Li, P. Li, and J. Yan, "Improve the flexibility provided by combined heat and power plants (CHPs) – a review of potential technologies," *e-Prime-Advances in Electrical Engineering, Electronics and Energy*, vol. 1, article 100023, 2021.

[14] M. S. Bakare, A. Abdulkarim, M. Zeeshan, and A. N. Shuaibu, "A comprehensive overview on demand side energy management towards smart grids: challenges, solutions, and future direction," *Energy Informatics*, vol. 6, no. 1, 2023.

[15] A. A. A. Radwan and Y. A.-R. I. Mohamed, "Grid-connected wind-solar cogeneration using back-to-back voltage-source converters," *IEEE Transactions on Sustainable Energy*, vol. 11, no. 1, pp. 315–325, 2020.

[16] M. Teymouri, S. Sadeghi, M. Moghimi, and S. Ghandehariun, "3E analysis and optimization of an innovative cogeneration system based on biomass gasification and solar photovoltaic thermal plant," *Energy*, vol. 230, article 120646, 2021.

[17] Q. Chen, M. Burhan, F. H. Akhtar et al., "A decentralized water/electricity cogeneration system integrating concentrated photovoltaic/thermal collectors and vacuum multi-effect membrane distillation," *Energy*, vol. 230, article 120852, 2021.

[18] Z. Wang, S. Sun, X. Lin et al., "A remote integrated energy system based on cogeneration of a concentrating solar power plant and buildings with phase change materials," *Energy Conversion and Management*, vol. 187, pp. 472–485, 2019.

[19] Y. He, S. Guo, J. Zhou, F. Wu, J. Huang, and H. Pei, "The many-objective optimal design of renewable energy cogeneration system," *Energy*, vol. 234, article 121244, 2021.

[20] M. K. Parizi, F. Keynia, and A. K. Bardsiri, "Woodpecker mating algorithm (WMA): a nature-inspired algorithm for solving optimization problems," *International Journal of Nonlinear Analysis and Applications*, vol. 11, no. 1, pp. 137–157, 2020.

[21] R. Choudhary, J. N. Rai, and Y. Arya, "Cascade FOPI-FOPTID controller with energy storage devices for AGC performance advancement of electric power systems," *Sustainable Energy Technologies and Assessments*, vol. 53, no. Part C, article 102671, 2022.

[22] D. Yadav, N. Singh, V. S. Bhadoria, N. C. Giri, and M. Cherukuri, "A novel metaheuristic jellyfish optimization algorithm for parameter extraction of solar module," *International Transactions on Electrical Energy Systems*, vol. 2023, article 5589859, pp. 1–21, 2023.

[23] M. Golam, R. Akter, J.-M. Lee, and D.-S. Kim, "A long short-term memory-based solar irradiance prediction scheme using meteorological data," *IEEE Geoscience Remote Sensing Letters*, vol. 19, article 1003705, 2022.

[24] B. K. Reddy and A. K. Singh, "Reactive power management and protection coordination of distribution network with high solar photovoltaic penetration," in *2021 12th International Renewable Engineering Conference (IREC)*, Amman, Jordan, 2021.

[25] G. Sharma, N. Krishnan, Y. Arya, and A. Panwar, "Impact of ultra-capacitor and redox flow battery with Jaya optimization for frequency stabilization in linked photovoltaic-thermal system," *International Transactions on Electrical Energy Systems*, vol. 31, no. 5, 2021.

[26] N. V. Quynh, Z. M. Ali, M. M. Alhaider, A. Rezvani, and K. Suzuki, "Optimal energy management strategy for a renewable-based microgrid considering sizing of battery energy storage with control policies," *International Journal of Energy Research*, vol. 45, no. 4, pp. 5766–5780, 2021.

[27] S. Kallio and M. Siroux, "Hybrid renewable energy systems based on micro-cogeneration," *Energy Reports*, vol. 8, no. 1, pp. 62–769, 2022.

[28] A. S. Al-Ezzi and M. N. M. Ansari, "Photovoltaic solar cells: a review," *Applied System Innovation*, vol. 5, no. 4, 2022.

[29] S. J. Yaqoob, A. L. Saleh, S. Motahhir, E. B. Agyekum, A. Nayyar, and B. Qureshi, "Comparative study with practical validation of photovoltaic monocrystalline module for single and double diode models," *Scientific Reports*, vol. 11, article 19153, 2021.

[30] S. Senthilkumar, V. Mohan, S. P. Mangaiyarkarasi, and M. Karthikeyan, "Analysis of single-diode PV model and optimized MPPT model for different environmental conditions," *International Transactions on Electrical Energy Systems*, vol. 2022, article 4980843, pp. 1–17, 2022.

[31] A. Memari, R. Ahmad, M. R. A. Jokar, and A. R. A. Rahim, "A new modified firefly algorithm for optimizing a supply chain network problem," *Applied Sciences*, vol. 9, no. 1, 2019.

[32] J. Lee, W. Wang, F. Harrou, and Y. Sun, "Reliable solar irradiance prediction using ensemble learning-based models: a comparative study," *Energy Conversion and Management*, vol. 208, article 112582, 2020.

[33] Y. Ma, Y. Han, M. Chen, and Y. Che, "Study on dynamic evaluation of Sci-tech journals based on time series model," *Applied Sciences*, vol. 12, no. 24, p. 12864, 2022.

[34] N. Bacanin, M. Zivkovic, T. Bezdan, K. Venkatachalam, and M. Abouhawwash, "Modified firefly algorithm for workflow scheduling in cloudedge environment," *Neural Computing & Applications*, vol. 34, no. 11, pp. 9043–9068, 2022.

[35] M. S. Alam, F. S. Al-Ismail, M. S. Hossain, and S. M. Rahman, "Ensemble machine-learning models for accurate prediction of solar irradiation in Bangladesh," *Processes*, vol. 11, no. 3, p. 908, 2023.